Journal of Molecular Liquids 211 (2015) 40–47

Contents lists available at ScienceDirect

Journal of Molecular Liquids

journal homepage: www.elsevier.com/locate/molliq

Density functional study of inclusion complex of Albendazole/cucurbit [7]uril: Structure, electronic properties, NBO, GIAO and TD-DFT analysis

Merabet Nora, Madi Fatiha, Nouar Leila *, Haiahem Sakina, Khatmi DjamelEddine

Laboratory of Computational Chemistry and Nanostructures, Department of Material Sciences, Faculty of Mathematical, Informatics and Material Sciences, University of 08 Mai 1945 Guelma, Algeria

ARTICLE INFO

Article history:
Received 10 May 2015
Received in revised form 15 June 2015
Accepted 17 June 2015
Available online 1 July 2015

Keywords:
Cucurbit [7]uril
Albendazole
DFT
NBO
GIAO
TD-DFT

ABSTRACT

In the present work, we investigate theoretically, the structure and electronic properties of inclusion complex of cucurbit [7]uril(Q[7]) with Albendazole (ABZ) using DFT calculations. Two modes of complexation were taken into consideration and the effect of solvent is explicitly taken into account. The results obtained with B3LYP/6-31G (d) method clearly indicate that the complexes formed are energetically favored with or without solvent. C1 complex (Albendazole entering the cavity of Q[7] by propyl and aromatic groups) is found more favored than C2 complex (Albendazole entering the cavity of Q[7] by carbamate group). ^{1}H nuclear magnetic resonance (NMR) was calculated by the Gauge-Including Atomic Orbital method and compared with available experimental data. Finally, TD-DFT calculations of visible spectra were analyzed and discussed. The theoretical calculation agrees well with that obtained from experimental data.

1. Introduction

Albendazole (ABZ) (Fig. 1a) which is chemically known as methyl[5-(propylthio)-1H-benzoimidazol-2-yl]carbamate has potent antiproliferative activity, and its clinical application as an anti-cancer agent is limited by its low aqueous solubility [1–7]. In order to increase the solubility of Albendazole and to use it in complex form, Na'il Saleh et al. [8] have prepared and characterized the encapsulation of ABZ in Q[7] by NMR and FT-IR techniques. The results indicate that the ABZ molecule is partially entrapped in the Q[7] cavity. However, the results obtained from ^{1}H NMR spectroscopy are not enough to describe the nature of intermolecular binding. So to complement these results, theoretical studies based on the density functional theory must be carried out to give a definitive geometry to the inclusion complex.

Cucurbit[n]uril (CB[n], n = 5, 6, 7, 8) is a relatively new family of macrocyclic host molecules. They are rigid macrocycles with unique cavities rimmed by carbonyl oxygens [8–10]. The use of cucurbit[n]urils (Q) macrocycles [11–13] in drug developments has attracted attention over the recent years [14,15] due to their distinct properties when compared to other classes of delivery vehicles such as dendimers, nanoparticles, or carbon nanotubes. Out of Q[n]s (n = 5, 6, 7 and 8). The Q[7] (Fig. 1b) host has been of particular interest in recent years because of its superior solubility in aqueous solution compared to other Q[n] members and its remarkable ability to form host–guest complexes [16]. Additionally, Q[7] is characteristic of low toxicity, high chemical and thermal stability [17]. There are many reports available in open literature exploring Q[7] as a successful host molecule [18,19]. Q[7] forms 1:1 complex with large number of guest molecules with very high association equilibrium in aqueous solution [16].

In this paper, we have investigated the inclusion processes of ABZ into Q[7] cavity using a B3LYP/6-31G(d) level of theory with the aim to give some insights about the geometry, electronic properties and the driving forces governing the formation of the inclusion complex.

2. Methodology

The quantum mechanical calculations were carried out at the density functional theory incorporating the Beck's three-parameter [20] exchange coupled with Lee et al.'s (B3LYP) correlation functional [21] which were obtained employing Gaussian 09 program [22].

The hybrid functional B3LYP has shown to be highly successful for calculation the electronic properties such as ionization potentials, electronic states and energy gaps [20–22]. The structures of ABZ and Q[7] were constructed using Hyperchem 7.5 molecular modeling package [23]. The penetration of ABZ in the cavity of the Q[7] can be done according two models. The model in which ABZ entering into the cavity of the Q[7] by propyl and aromatic groups was called the "C1 complex", the other in which ABZ entering into the cavity of the Q[7] by carbamate group was called the "C2 complex" (Fig. 2).

For the DFT calculations, no constraints were imposed on the whole system, especially no parameters were fixed. So the ABZ molecule was

* Corresponding author.
E-mail address: leilanoua@yahoo.fr (N. Leila).

http://dx.doi.org/10.1016/j.molliq.2015.06.054

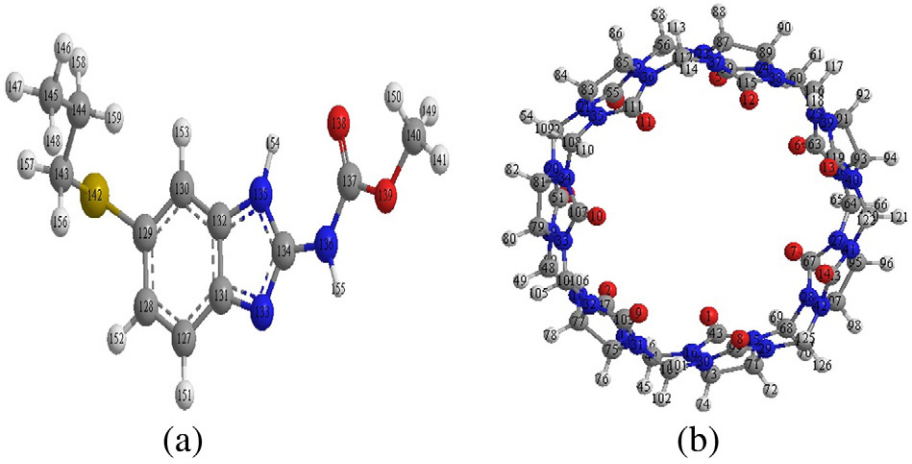

Fig. 1. Geometrical structures of ABZ (a) and Q[7] (b) optimized at B3LYP/6-31G(d) method. Atomic numbering of ABZ and Q[7].

free to move in the cavity of the Q[7] during the whole optimization process. Therefore, conformational changes of the host as well as of the guest molecule were explicitly allowed. The complexation energy (ΔE) between ABZ and Q[7] was calculated for the minimum energy structure according to the following:

$$\Delta E = E_{complex} - (E_{free\ ABZ} + E_{free\ Q[7]}) \quad (1)$$

where $E_{complex}$, $E_{Q[7]}$, and $E_{free\ ABZ}$ represent respectively the total energy of the complex, the free optimized Q[7], and the free optimized ABZ energy. The deformation energy of the guest or the host molecule can be obtained by Eqs. (2) and (3):

$$E_{deformation}(Guest) = E[Guest]_{sp}^{opt} - E[Guest]_{opt} \quad (2)$$

where $E_{deformation}(Guest)$ stands for the deformation energy of the guest, $E[Guest]_{sp}^{opt}$ is the single point energy of the guest using its geometry in the optimized complex, and $E[Guest]_{opt}$ is the energy of the optimized geometry of the guest.

$$E_{deformation}(Host) = E[Host]_{sp}^{opt} - E[Host]_{opt} \quad (3)$$

where $E_{deformation}(Host)$ stands for the deformation energy of the guest, $E[Host]_{sp}^{opt}$ is the single point energy of the guest using its geometry in the optimized complex, and $E[Host]_{opt}$ is the energy of the optimized geometry of the guest.

It is important to know the effect of water molecules on the stability of the ABZ/Q7 complex, so the geometries obtained by DFT calculations in vacuum of the complexes were optimized in water. We represented the solvent implicitly by calculation polarized continuum model (CPCM) [24]. B3LYP calculations using the 6-31G(d) basis set was generally consistent with the experiments and provide valuable data to complement the experimental work, while the agreement with experiment also increases our confidence in the computational results.

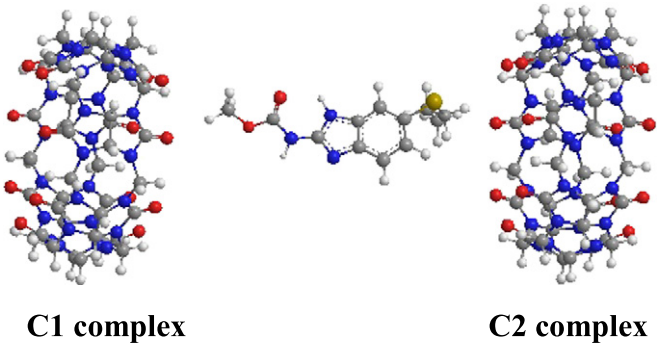

Fig. 2. The proposed structures of CBZ/Q[7] complex for C1 and C2 complexes.

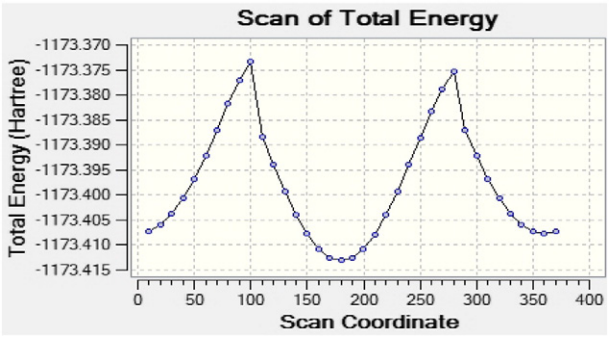

Fig. 3. Scan of total energy of θ2 ($C_{134}N_{136}C_{137}O_{139}$) torsional angle calculated by B3LYP/6-31G(d) method.

Table 1
Complexation energies, DEF, dipole moment, HOMO, LUMO, Δ(HOMO − LUMO), chemical potential (μ), electronegativity (χ), softness (S), hardness (η) and electrophilicity (ω) of the ABZ, CB[7] and inclusion complexes in vacuum calculated by B3LYP/6-31G(d) method.

In vacuum				
	ABZ	Q[7]	C1 complex	C2 complex
E (kcal/mol)	−739,982.49	−2,643,200.44	−3,383,194.87	−3,383,195.46
ΔE (kcal/mol)			−11.94	−12.53
DEF (ABZ) (kcal/mol)			−0.68	−0.50
DEF (Q[7]) (kcal/mol)			−9.99	−10.01
D (Debye)	4.50	0.004	5.56	5.61
HOMO (eV)	−5.69	−6.48	−4.33	−4.07
LUMO (eV)	−0.57	0.72	0.63	0.63
Δ(HOMO − LUMO) (eV)	−5.12	−7.20	−4.96	−4.70
μ (eV)	−3.13	−2.88	−1.85	−1.72
χ (eV)	3.13	2.88	1.85	1.72
S (eV)	0.39	0.27	0.40	0.42
η (eV)	2.56	3.60	2.48	2.35
ω (eV)	1.91	1.15	0.69	0.63

Table 2
Complexation energies, DEF, dipole moment, HOMO, LUMO, Δ(HOMO − LUMO), chemical potential (μ), electronegativity (χ), softness (S), hardness (η) and electrophilicity (ω) of the ABZ, Q[7] and inclusion complexes in water calculated by B3LYP/6-31G(d) method.

In water				
	ABZ	Q[7]	C1 complex	C2 complex
E (kcal/mol)	−739,990.41	−2,643,271.47	−3,383,280.42	−3,383,280.52
ΔE (kcal/mol)			−18.54	−18.64
DEF (ABZ) (kcal/mol)			−7.33	−7.95
DEF (Q[7]) (kcal/mol)			−11.68	−11.33
D (Debye)	5.94	0.07	6.81	7.51
HOMO (eV)	−5.91	−6.69	−5.59	−5.53
LUMO (eV)	−0.73	0.53	−0.46	−0.47
Δ(HOMO − LUMO) (eV)	−5.18	−7.22	−5.13	−5.06
μ (eV)	−3.32	−3.08	−3.02	−3.00
χ (eV)	3.32	3.08	3.02	3.00
S (eV)	0.39	0.28	0.39	0.40
η (eV)	2.59	3.61	2.56	2.53
ω (eV)	2.13	1.31	1.78	2.53

After that, ^{1}H NMR calculations were carried out to quantify the chemical shifts of protons of Q[7], ABZ and their inclusion complex. The optimized molecular geometries was performed with the Gauge-Independent Atomic Orbital (GIAO) method and the B3LYP/6-31G(d) model chemistry. At last, the calculations of maximum visible absorption of the studied complexes were performed by the TD-DFT method.

3. Results and discussions

3.1. Conformational search

Before the creation of the inclusion complex, we have made a conformational search in order to find the global minimum of ABZ, the level with the B3LYP/6-31G(d) basis set was used to derive all theoretically possible conformer forms of the molecule. Six dihedral angles are taken into account, as follows: θ1 ($C_{134}N_{136}C_{137}O_{138}$), θ2 ($C_{134}N_{136}C_{137}O_{139}$), θ3 ($N_{136}C_{137}O_{139}C_{140}$), θ4 ($O_{138}C_{137}O_{139}C_{140}$), θ5 ($C_{129}S_{142}C_{143}C_{144}$) and θ6 ($S_{142}C_{143}C_{144}C_{145}$). For each angle the structure of ABZ was fully optimized with the B3LYP/6-31G(d) method.

To find a more stable structure for each angle, the energy calculation by scanning θ from 0° to 360° at 30° intervals was carried out. As shown in the supplementary figure, several stable energy conformers for ABZ were identified. The most stable conformer was obtained at 180° for dihedral angle θ2 (Fig. 3). Then, the lowest-energy structure found in the conformational searches was used as the starting structure to create Q[7] inclusion complexes.

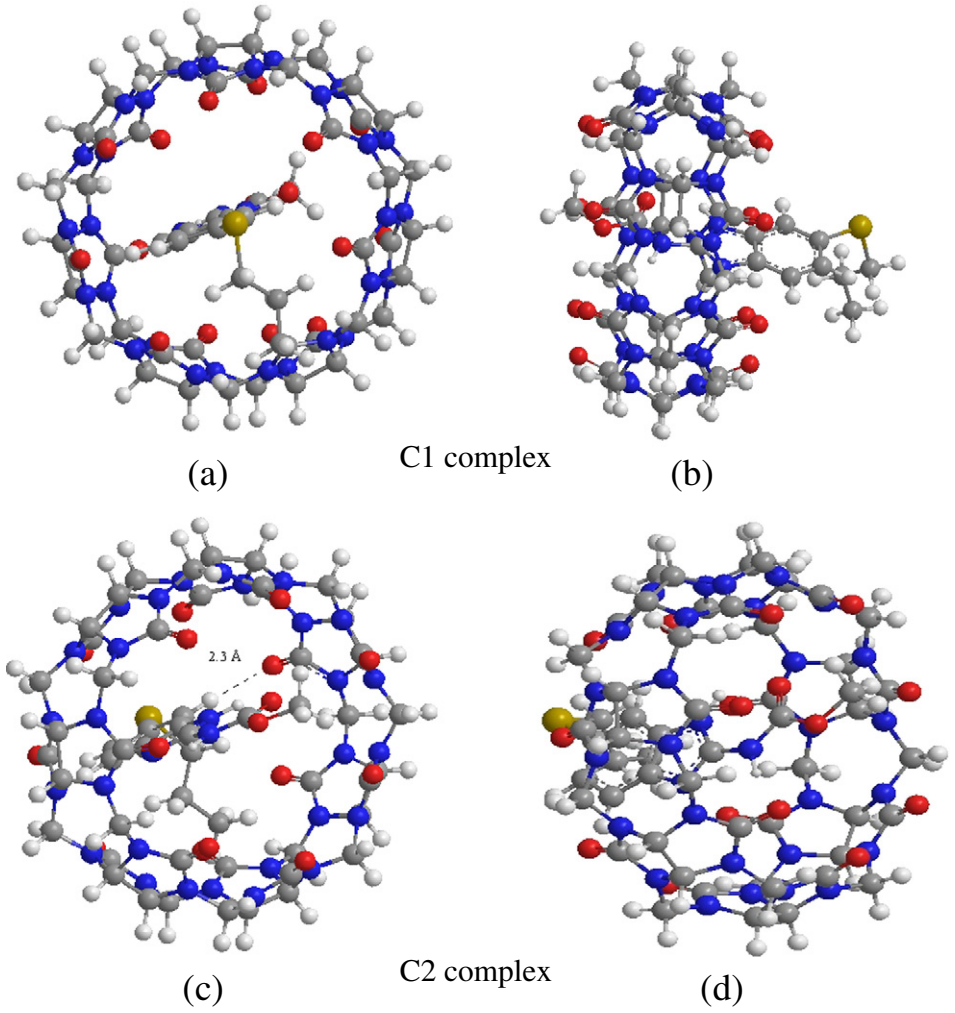

Fig. 4. B3LYP/6-31G(d) energy minimized structure of C1 complex for the (a) bird's eye-view, (b) side view and C2 complex for the (c) bird's eye-view, and (d) side view. Hydrogen bonds are indicated by dotted lines.

Table 3
Distances in Q[7] before and after inclusion with ABZ.

Distances	Free ABZ	Q[7] in C1 complex	Q[7] in C2 complex
O_7–O_3	8.5	8.2	7.8
O_9–O_{12}	8.5	8.9	7.8
C_{44}–C_{59}	10.5	10.6	10.8
C_{63}–C_{48}	10.5	10.2	10.1
N_{15}–N_{22}	10.6	10.7	10.9
N_{21}–N_{28}	10.6	10.5	10.5

3.2. Energies

Tables 1 and 2 summarize complexation energies, DEF, dipole moment (D), HOMO, LUMO, Δ(HOMO − LUMO), chemical potential (μ), electronegativity (χ), softness (S), hardness (η) and electrophilicity (ω) of the ABZ, Q[7] and inclusion complexes in vacuum and in water. From Tables 1 and 2, it can be seen that the negative complexation energy for the inclusion complexes indicate that the encapsulation processes in vacuum and in water are thermodynamically favorable in nature. The difference in complexation energy for the inclusion complexes in vacuum of ABZ with Q[7] between the two complexes C1 and C2 corresponds to −0.59 kcal/mol (Table 1). When the complexes take place in aqueous solution (Table 2); the complexation energies were found equal to −18.54 kcal/mol for C1 complex and to −18.64 kcal/mol for C2 complex; corresponding to a difference between the two complexes equal to 0.1 kcal/mol. The results of calculations listed in Table 2 confirm those obtained in vacuum (Table 1). The C2 complex in water is indeed significantly more favorable than the other complexes. These results agree with the experimental observations [8]. In addition, upon complexation, a remarkable distortion of the ABZ and the Q[7] molecules were detected. The results indicated that the deformation energy of the ABZ molecule in vacuum and in water is higher than that of Q[7] in C1 and C2 complexes. In water, the Q[7] molecule in C2 complex requires more energy than in the C1

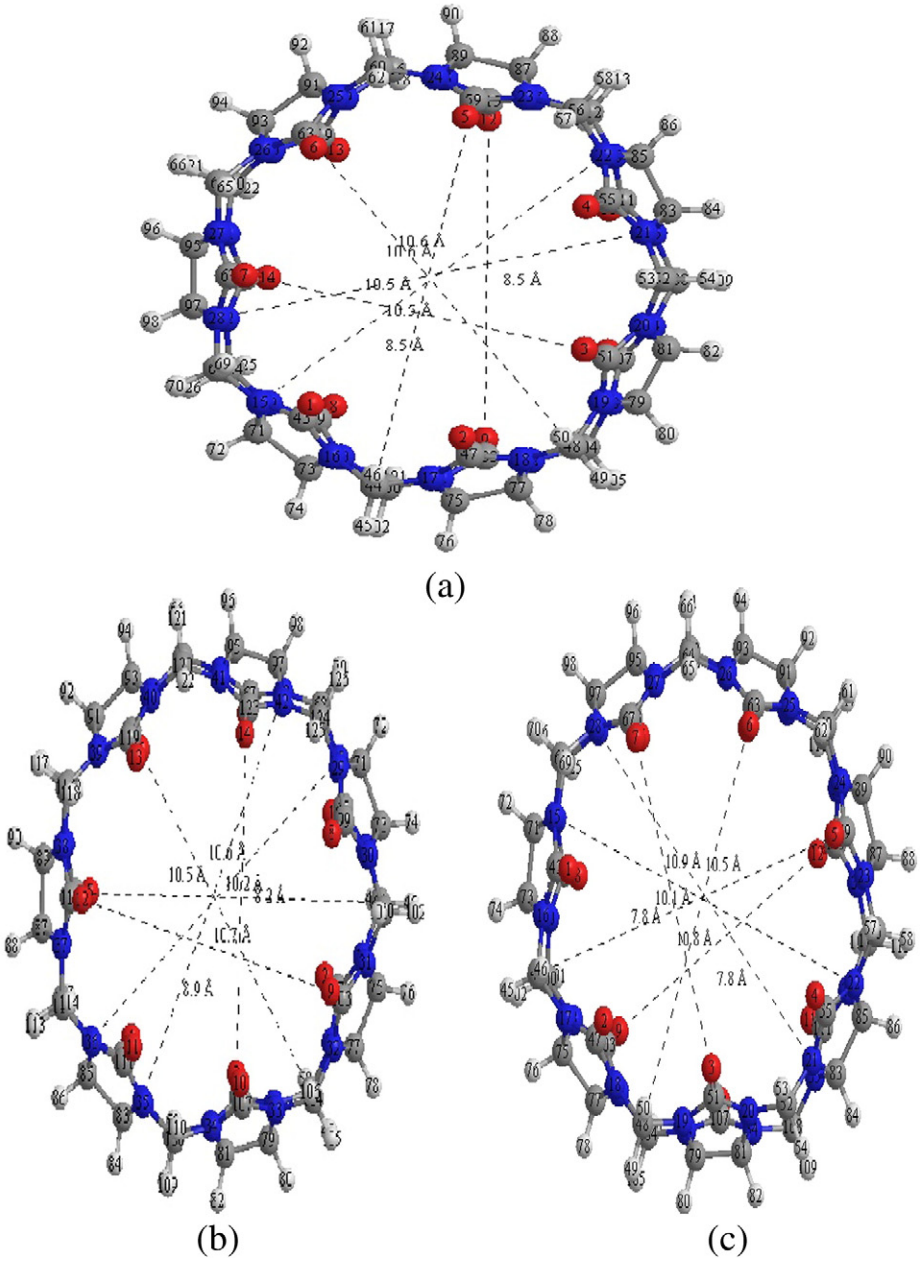

Fig. 5. B3LYP/6-31G(d) optimized structure of Q[7] free (a) and in C1 (b) and C2 (c) complexes. The dotted line length represents the distance between numbered atoms.

complex. In contrast, ABZ molecule in C1 complex requires slightly more energy than for C2 complex in order to adapt its structure to bind within the cavity of Q[7]. From Tables 1 and 2, we noticed that all the inclusion complexes in vacuum and in water showed dipole moment values higher than the corresponding isolated molecules. The augmentation of the polarity of the Q[7] indicates the formation of complexes. From these results it can be concluded that the dipole moment values show a strong correlation with the complexation behavior of the molecules.

3.3. Geometric parameters

The B3LYP/6-31G(d) optimized geometries of ABZ/Q[7] inclusion complexes in water are presented in Fig. 4. The structural analysis of C2 complex show the presence of one hydrogen bonds formed between hydrogen atom H (153) of ABZ and oxygen atom O (1) of Q[7] with a distance of 2.3 Å (see Fig. 4b). In the case of C1 complex no H-bond was found, this explains why the complexation energy of the inclusion in the C2 complex is lower than that of the C1 complex (see Fig. 4a). Upon examining the optimized geometries of C1 and C2 complexes in water, we notice that the ABZ molecule is inserted partially into the cavity of Q[7]. In C2 complex, the carbamate group is located outside of the Q[7] portal, whereas the propyl and aromatic groups are located within the Q[7] cavity. In C1 complex the carbamate methyl is located inside of the Q[7] cavity. The proposed inclusion complex with Albendazole for C2 complex in water in agreement with the experimental observations [8].

The structural parameters of the host molecule before and after complexation obtained from the B3LYP/6-31G(d) calculations in water are summarized in Table 3 and Fig. 5. Upon complexation, a remarkable distortion of the Q[7] molecule was detected. This one was confirmed by comparing the variation of the mean distances between the nitrogen, carbon and oxygen atoms. As can be seen in Table 3 the distances are changed after inclusion of ABZ into Q[7] cavity. The N_{15}–N_{22} distance is increased after complexation with ABZ, the difference is 0.1 Å for C1 and C2 complexes. In the case of C_{63}–C_{48} distance, the initial value is of 10.5 Å after inclusion it become 10.2 Å for C1 complex and 10.1 Å for C2 complex. For C_{44}–C_{59} distance become longer after interaction with ABZ the difference is about 0.1 Å for C1 complex and about 0.3 for C2 complex. Also for O_7–O_3 distance (8.5 Å), after inclusion it become 8.2 Å and 7.8 Å for C1 and C2 complexes respectively. The geometrical changes of Q[7] before and after guest inclusion are shown in Fig. 5a–c. The round cavity (Fig. 5a) of Q[7] turns into a deformed shaped cavity (Fig. 5b, c). It is interesting to note A great deformation of Q[7] in C2 complex when compared to in C1 complex. This indicates that Q[7] in C2 complex adopts a specific conformation to form stable inclusion complex with ABZ. This result is confirmed by the deformation energy (see Tables 1 and 2). From these results we conclude, that the nitrogen, carbon and oxygen atoms play a significant role in binding the ABZ.

3.4. Electronic and charge properties

The results of the HOMO and LUMO energies of the isolated host, guest and their complexes are summarized in Tables 1 and 2. The LUMO as an electron acceptor represents the ability to obtain an electron and HOMO represents the ability to donate electron. The most important terms in this kind of interaction are contributed from the partial charge transfer between the HOMO of one component and the LUMO of another. The ($E_{HOMO} - E_{LUMO}$) gap is an important scale of stability [25] and chemicals with large ($E_{HOMO} - E_{LUMO}$) values tend to have higher stability. The Δ ($E_{HOMO} - E_{LUMO}$) of the C2 complex (in vacuum and in water) was higher than that of C1 complex. Fig. 6 illustrates the HOMO and LUMO energy orbital pictures of C1 and C2 complexes in water. These results indicate that the HOMO orbital is localized on the benzimidazole ring and propylthio group of ABZ and the LUMO orbital is observed on the Q [7].

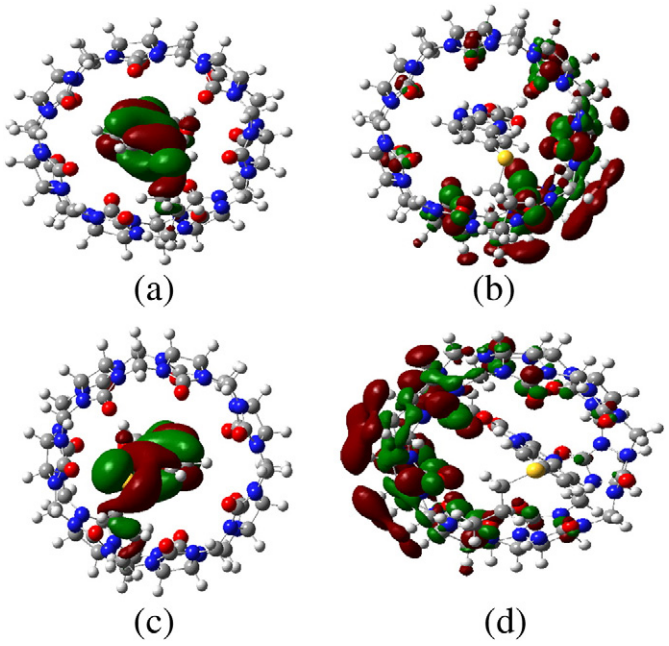

Fig. 6. Typical contour plots of HOMO and LUMO respectively of C1 complex (a), (c) and C2 complex (b), (d) in water.

The global indices of reactivity are presented in Tables 1 and 2. The value of electronic chemical potential μ, electronegativity χ, softness S, hardness η and electrophilicity ω for complexes is differing from the individual host and guest molecules. (i) The chemical potential of all the inclusion complexes are negative which indicates that all the inclusion process are spontaneous. (ii) The global hardness (η) of the C1 and C2 complexes decreased after the ABZ penetrate into the cavity of the Q [7]. (iii) Softness of the C2 complex in vacuum and in water is higher than that of the C1 complex. (iv) ω is an important index of electrophilicity and large values are characteristics of most electrophilic systems. Based on this reasoning, we can conclude, from the results, that the C2 complex in water is qualified as the most electrophilic. On the other hand, the charge transfer interactions play a relevant role in the stabilization of the inclusion complexes. The calculated of the NBO charges of the heavy atoms for the free ABZ, charge transfer of C1 and C2 complexes are summarized in Table 4. As it could be observed in Table 4, that the partial charge of the atoms of ABZ was significantly changed during the complexation. Charge distribution reveals that the charges

Table 4
Mulliken charges of the atoms of ABZ, charge transfer of the C1 and C2 complexes by NBO calculations.

Atom no.	Free ABZ	ABZ in C1 complex	ABZ in C2 complex
C127	−0.055	−0.037	−0.033
C128	−0.017	−0.034	−0.044
C129	−0.119	−0.114	−0.118
C130	−0.031	−0.012	−0.004
C131	0.240	0.232	0.229
C132	0.362	0.338	0.338
N133	−0.614	−0.620	−0.620
C134	0.758	0.757	0.756
N135	−0.353	−0.362	−0.363
N136	−0.345	−0.349	−0.355
C137	0.834	0.831	0.833
O138	−0.544	−0.543	−0.542
O139	−0.475	−0.480	−0.480
C140	0.333	0.304	0.307
S142	0.013	0.001	−0.004
C143	−0.036	−0.053	−0.051
C144	0.042	0.050	0.048
C145	0.006	−0.008	−0.012

Table 5
Donor–acceptor interactions and stabilization energies $E^{(2)}$ (kcal/mol) of ABZ/Q[7] in water.

Donor	Acceptor	$E^{(2)}$ B3LYP/31G(d)	Å
C1 complex			
LP(O1)	σ* (C 140–H 149)	0.56	2.5
LP(O2)	σ* (C 140–H 150)	0.63	2.6
LP(O8)	σ* (C 130–H 153)	0.75	2.5
LP(O12)	σ* (C 127–H 151)	1.26	2.5
Total		3.20	
C2 complex			
LP(O1)	σ* (C 130–H 153)	2.01	2.3
LP(O2)	σ* (C 143–H 156)	0.59	2.7
LP(O5)	σ* (C 127–H 151)	0.54	2.5
LP(O14)	σ* (C 140–H 150)	0.76	2.5
Total		3.90	

of some atoms C128, N133, N136 and C145 of the ABZ in C1 and C2 complexes are more negative than those in isolated form; while others atoms such C144, is more positive than those in the isolated ABZ. In C137, C131 and C132 charges of the atoms of ABZ were decreased after complexation. This means that when the guest molecule interacts with Q[7], its charge distribution changes.

3.5. NBO analysis

The natural bonding orbital (NBO) analysis was applied for investigating the hydrogen bond (donor–acceptor interactions) in the complexes of ABZ with Q[7]. Table 5 shows some of the significant donor–acceptor interactions and their stabilization energies $E^{(2)}$. The interaction energies of these contacts are in the range of 0.56–1.26 kcal/mol in C1 complex and 0.54–2.01 kcal/mol in C2 complex. The obtained stabilization energies $E^{(2)}$ from B3LYP/6-31G(d) were 3.2 and 3.9 kcal/mol for C1 and C2 complexes respectively. Thus, the encapsulation of ABZ with Q[7] for C1 (3.2 Kcal/mol) complex is less demanding in energy than C2 (3.9 Kcal/mol) one. The structures of the energy minimum obtained with B3LYP/31G(d) calculations show the presence of several intermolecular hydrogen bond interactions as shown in Fig. 7. In C1 complex, when ABZ plays the role of acceptor, the important interaction is observed between LP(O12) and σ* C 127–H 151 (1.26 kcal/mol, 2.5 Å). For C2 complex, the greater interaction is formed between LP(O1) and σ* C130–H153 (2.01 kcal/mol, 2.3 Å). In addition, the implicated orbitals in donor acceptor interaction of ABZ in C2 complex are mainly of benzimidazole ring. The intermolecular distances between occupied and unoccupied orbital's given in NBO analysis of the two molecules are as follows: (i) O1 — H 153: 2.3 Å; (ii) O2 — H 156: 2.7 Å; (iii) O5 — H 151: 2.5 Å and (iv) O14 — H 150: 2.5 Å. Thus, the benzimidazole ring is closed to internal behavior of CB[7], which explains the upfield shifts for the ABZ propyl and benzimidazole resonances observed experimentally [8]. The encapsulation of benzimidazole ring into CB [7] cavity is found theoretically for carbendazim/CB[7] inclusion complex by B3LYP/631G and HF/6-31G calculations [18].

3.6. GIAO/DFT calculation

The Gauge-Including Atomic Orbital (GIAO) method as implemented in Gaussian 09 was employed for ^{1}H NMR calculations and by employing the density functional theory B3LYP at 6-31G* basis set with using corresponding TMS shielding calculated at the same theoretical level as the reference. The solvent effects have been investigated using the CPCM method for water as a solvent (ε = 78.35) [26]. ^{1}H NMR calculations of isolated ABZ and C2 complex in water are presented in Table 6. NMR chemical shifts (δ) are calculated by subtracting the nuclear magnetic shielding tensors of protons in molecules of interest from those in teramethyl silane, TMS (as a reference), using the gauge invariant atomic orbital method. Inclusion of ABZ in Q[7] cavity is put in evidence by the change in chemical shifts of some of the guest protons, in comparison with the chemical shifts of the same protons in the free component. In Table 6, we reported and compared the values of NMR chemical shifts (δ) computed with B3LYP/6-31G* method to those obtained from experimental data. As can be seen from Table 6, the protons signals of H151 and H157 of ABZ after complexation shifted to a large field. Whereas the signals of the other protons of ABZ have lowest chemical shifts changes. From Table 6, the largest difference between the theoretical chemical shifts and experimental chemical shifts is seen in protons H_{153}. The possible cause of this difference is the hydrogen bonds formed between hydrogen atom H (153) of ABZ and oxygen atom O (1) of Q[7]. According to the theoretical data from the Gauge-Including Atomic Orbital (GIAO) method and the experimental data from ^{1}H NMR we can conclude that Q[7] forms an inclusion complex with ABZ, where only the carbamate methyl is located outside of the Q[7] portal, whereas the propyl and aromatic groups are located within the Q7 cavity.

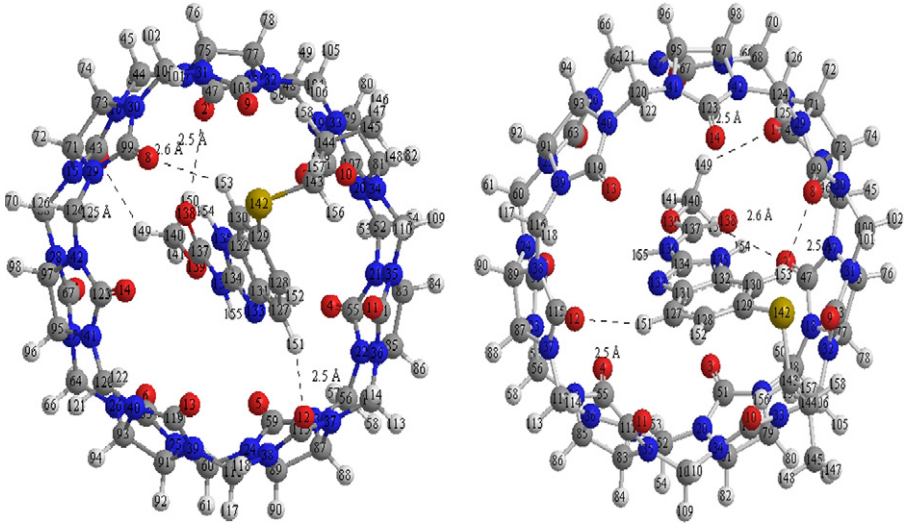

Fig. 7. The hydrogen bonds in C1 and C2 complexes in water.

Table 6
Calculated NMR shifts.

^{1}H-shift of atom (ppm)	ABZ	$\delta_{ABZ\ in\ C2\ complex}$	$\delta_{Experimental}$ [8]	Δδ
H_{151}	7.25	7.76	7.30	0.46
H_{152}	7.37	7.21	6.50	0.71
H_{153}	7.48	7.95	6.50	1.45
H_{157}	2.78	2.46	2.10	0.36
H_{158}	1.72	1.62	0.90	0.72
H_{147}	0.94	0.87	0.10	0.77

$\Delta\delta = \delta_{ABZ\ in\ C2\ complex} - \delta_{Experimental}$.

3.7. UV–vis spectra

To investigate the nature of electronic transitions, the electronic spectra of the studied complexes were calculated using the time-dependent density functional theory (TD-DFT) approach at the B3LYP/6-31G(d) level on the basis of fully optimized ground-state structure. Calculations are performed in water at CPCM model [27]. All computational predictions of the UV–vis spectra are summarized in Fig. 8 and Table 7. For C1 complex, the absorption bands are observed at 249 nm, 255 nm and 270 nm. The absorption band at 249 nm having oscillator strength of 0.305. In this excitation, the H-2 → L (4.21%) and H → L (86.38%) configurations are responsible for this absorption. The band at 255 nm has oscillator strength of 0.001 and vertical excitation energy equal to 4.896 eV. For the third band at 270 nm the vertical excitation energy equal to 5.055 eV. For C2 complex, the absorption bands are observed at 240 nm, 258 nm and 280 nm. The absorption band at 280 nm having oscillator strength of 0.120 and vertical excitation energy equal to 5.084. H-2 → L (82.25%), H-1 → L + 1 (2.41%), H → L (5.19%) and H → L + 1 (3.59%) configurations can be responsible for this absorption.

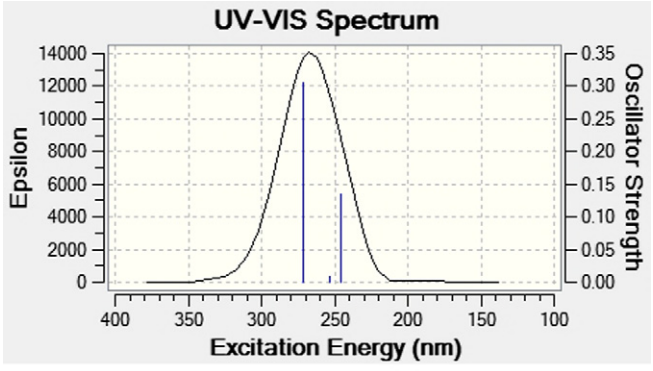

C1 complex

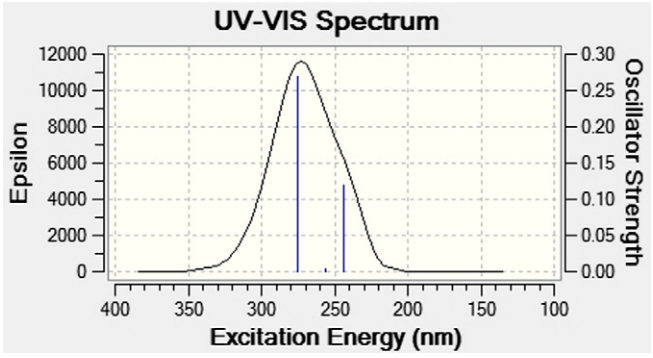

C2 complex

Fig. 8. TD-DFT calculated absorption spectra of C1 and C2 complexes.

Table 7
Vertical excitation energies (eV), oscillator strengths (f) and configurations of excitations.

		E (eV)	*f*	Configuration	Main attribution
Complex 1	Band 1	4.575	0.3052	H-2 → L (4.21%)	CBZ/Q[7]
				H → L (86.38%)	CBZ/Q[7]
	Band 2	4.8960	0.0082	H-2 → L (12.11%)	CBZ/Q[7]
				H-1 → L (44.04%)	CBZ/Q[7]
				H → L + 1 (38.89%)	CBZ/Q[7]
	Band 3	5.0554	0.1348	H-2 → L (74.60%)	CBZ/Q[7]
				H-2 → L + 1 (2.42%)	CBZ/Q[7]
Complex 2	Band 1	4.5033	0.2691	H-1 → L + 1 (2.07%)	CBZ/Q[7]
				H → L (89.45%)	CBZ/Q[7]
	Band 2	4.8450	0.0029	H-2 → L (4.12%)	CBZ/Q[7]
				H-1 → L (63.91%)	CBZ/Q[7]
	Band 3	5.0842	0.1197	H-2 → L (82.25%)	CBZ/Q[7]
				H-1 → L + 1 (2.41%)	CBZ/Q[7]
				H → L (5.19%)	CBZ/Q[7]
				H → L + 1 (3.59%)	CBZ/Q[7]

4. Conclusion

The complexation of Albendazole with cucurbit [7]uril was studied by density functional B3LYP/6-31G(d) calculations. Structure, electronic properties, NBO, ^{1}H NMR and UV–vis were analyzed. The result suggests that the complexation energy of the C2 complex in water is significantly more favorable than the others. Upon complexation, a remarkable distortion of the Q[7] molecule was detected. NBO analysis show that the hydrogen bonding between the portal oxygen atom of Q[7] and the hydrogen atom of ABZ are the major factors contributing to the stabilities of the complexes. The theoretical calculation agrees well with that obtained from experimental data.

Acknowledgments

This study was supported by the Algerian Ministry of Higher Education and Scientific Research and the General Direction of Scientific Research as part of the projects CNEPRU (Nos B01520090002 and E01520140081).

Appendix A. Supplementary data

Supplementary data to this article can be found online at http://dx.doi.org/10.1016/j.molliq.2015.06.054.

References

[1] N. Desilva, H. Guyatt, D. Bundy, Anthelmintics, J. Drugs 53 (1997) 769–788.
[2] S. Torrado, S. Torrado, J.J. Torrado, R. Cardoniga, Preparation, dissolution and characterization of albendazole solid dispersions, Int. J. Pharm. 140 (1996) 247–250.
[3] J.L. Del Estal, A.I. Alvarez, C. Villaverde, J.G. Prieto, Comparative effects of anionic, natural bile acid surfactants and mixed micelles on the intestinal absorption of the anthelmintic albendazole, Int. J. Pharm. 91 (1993) 105–109.
[4] H. Wen, R.R. New, M. Muhmut, Y.H. Wang, J.H. Zang, Y.M. Shao, P.S. Craig, Pharmacology and efficacy of liposome entrapped albendazole in experimental secondary alveolar echinococcosis and effect of co-administration with cimetidine, Parasitology 113 (Pt2) (1996) 111–121.
[5] M. Kata, M. Shauer, Increasing the solubility characteristics of albendazole with dimethyl-β-cyclodextrin, Acta Pharm. Hung. 61 (1991) 23–31.
[6] Yunjie Zhao, Damian P. Buck, David L. Morris, Mohammad H. Pourgholami, Anthony I. Day, J. Grant Collins, Solubilisation and cytotoxicity of albendazole encapsulated in cucurbit[*n*]uril, Org. Biomol. Chem. 6 (2008) 4509–4515.
[7] Yunjie Zhao, Damian P. Buck, David L. Morris, Mohammad H. Pourgholami, Anthony I. Day, J. Grant Collins, Solubilisation and cytotoxicity of albendazole encapsulated in cucurbit[*n*]uril, Org. Biomol. Chem. 6 (2008) 4509–4515.
[8] Na'il Saleh, Abbas Khaleel, Hmoud Al-Dmour, Bassam al-Hindawi, Elena Yakushenko, Host–guest complexes of cucurbit [7]uril with albendazole in solid state. Thermal and structural properties, J. Therm. Anal. Calorim. 111 (2013) 385–392.
[9] J.W. Lee, S. Samal, N. Selvapalam, H.-J. Kim, K. Kim, Cucurbituril homologues and derivatives: new opportunities in supramolecular chemistry, Acc. Chem. Res. 36 (2003) 621–630.
[10] A. Day, A.P. Arnold, R.J. Blanch, B. Snushall, Supramolecular systems in biomedical fields, J. Org. Chem. 66 (2001) 8094–8100.

[11] E.G. Shchepotina, E.A. Pashkina, E.V. Yakushenko, V.A. Kozlov, Cucurbiturils as containers for medicinal compounds, Nanotechnol. Russ. 6 (2011) 11–12.
[12] Indrajit Ghosh, Werner M. Nau, The strategic use of supramolecular pKa shifts to enhance the bioavailability of drugs, Adv. Drug Deliv. Rev. 64 (2012) 764–783.
[13] E. Shchepotina, E. Pashkina, E. Yakushenko, V. Kozlov, Cucurbiturils as containers for medicinal compounds, Nanotechnol. Russ. 6 (11) (2011) 773–779 (35).
[14] Y.P. Li, H. Wu, L.M. Du, Chin, Study on the inclusion interactions of berberine hydrochloride and cucurbit[7] by spectrofluorimetry, Chem. Lett. 20 (2009) 322–325.
[15] M. Megyesi, L. Biczok, I. Jablonkai, Highly sensitive fluorescence response to inclusion complex formation of berberine alkaloid with cucurbit [7] uril, J. Phys. Chem. 112 (2008) 3410–3416.
[16] Ruibing Wang, Donal H. Macartney, Cucurbit[7]uril stabilization of a diarylmethane carbocation in aqueous solution, Tetrahedron Lett. 49 (2008) 311–314.
[17] Liyun Maa, Si-Min Liub, Lin Yaoa, Li Xua, Preparation and chromatographic performance evaluation of cucurbit[7]uril immobilized silica, J. Chromatogr. A 1376 (2015) 64–73.
[18] Madi Fatiha, Bounefla Faiza, Kirati Ichraf, Nouar Leila, Khatmi DjamelEddine, TD-DFT calculations of visible spectra and structural studies of carbendazim inclusion complex with cucurbit[7]uril, J. Taiwan Inst. Chem. Eng. 000 (2015) 1–6.
[19] M. del Pozo, L. Hernández, C. Quintana, A selective spectrofluorimetric method for carbendazim determination in oranges involving inclusion-complex formation with cucurbit[7]uril, Talanta 81 (2010) 1542–1546.
[20] A.D. Becke, Density-functional exchange-energy approximation with correct asymptotic behavior, Phys. Rev. A38 (1988) 3098–3100.
[21] C. Lee, W. Yang, R.G. Parr, Development of the Colle–Salvetti correlation-energy formula into a functional of the electron density, Phys. Rev. B 37 (1988) 785–789.
[22] M.J. Frisch, G.W. Trucks, H.B. Schlegel, G.E. Scuseria, M.A. Robb, J.R. Cheeseman, G. Scalmani, V. Barone, B. Mennucci, G.A. Petersson, H. Nakatsuji, M. Caricato, X. Li, H.P. Hratchian, A.F. Izmaylov, J. Bloino, G. Zheng, J.L. Sonnenberg, M. Hada, M. Ehara, K. Toyota, R. Fukuda, J. Hasegawa, M. Ishida, T. Nakajima, Y. Honda, O. Kitao, H. Nakai, T. Vreven, J.A. Montgomery Jr., J.E. Peralta, F. Ogliaro, M. Bearpark, J.J. Heyd, E. Brothers, K.N. Kudin, V.N. Staroverov, R. Kobayashi, J. Normand, K. Raghavachari, A. Rendell, J.C. Burant, S.S. Iyengar, J. Tomasi, M. Cossi, N. Rega, J.M. Millam, M. Klene, J.E. Knox, J.B. Cross, V. Bakken, C. Adamo, J. Jaramillo, R. Gomperts, R.E. Stratmann, O. Yazyev, A.J. Austin, R. Cammi, C. Pomelli, J.W. Ochterski, R.L. Martin, K. Morokuma, V.G. Zakrzewski, G.A. Voth, P. Salvador, J.J. Dannenberg, S. Dapprich, A.D. Daniels, O. Farkas, J.B. Foresman, J.V. Ortiz, J. Cioslowski, D.J. Fox, Gaussian 09, Revision A.02, Gaussian, Inc., Wallingford CT, 2009.
[23] Hyperchem Release 7.51 for Windows 2002, Hypercube, Inc., 2002
[24] Haizhen Zhang, Tyler A. Ferrell, Matthew C. Asplund, David V. Dearden, Molecular beads on a charged molecular string: α, ω-alkyldiammonium complexes of cucurbit[6]uril in the gas phase, Int. J. Mass Spectrom. 265 (2007) 187–196.
[25] Ambigapathy Suvitha, Natarajan Sathiyamoorthy Venkataramanan, Hiroshi Mizuseki, Yoshiyuki Kawazoe, Nobiaki Ohuchi, Theoretical insights into the formation, structure, and electronic properties of anticancer oxaliplatin drug and cucurbit [n]urils n = 5 to 8, J. Incl. Phenom. Macrocycl. Chem. 66 (2010) 213–218.
[26] Djilani Imene, Madi Fatiha, Nouar Leila, Haiahem Sakina, Rahim Mohamed, Khatmi DjamelEddine, Bouhadiba Abdelaziz, Theoretical investigation to characterize the inclusion complex of a-lipoic acid and β-cyclodextrin, C. R. Chim. 18 (2015) 170–177.
[27] Feifei Chen, Yujiao Wang, Xiaomei Xie, Meng Chen, Wei Li, TDDFT study of UV–vis spectra of permethrin, cypermethrin and their beta-cyclodextrin inclusion complexes: a comparison of dispersion correction DFT (DFT-D3) and DFT, Spectrochim. Acta A Mol. Biomol. Spectrosc. 128 (2014) 461–467.